IEEE Access
Multidisciplinary | Rapid Review | Open Access Journal

SPECIAL SECTION ON MILLIMETER-WAVE COMMUNICATIONS: NEW RESEARCH TRENDS AND CHALLENGES

Received March 28, 2019, accepted April 30, 2019, date of publication May 3, 2019, date of current version May 21, 2019.

Digital Object Identifier 10.1109/ACCESS.2019.2914685

Hand Grip Impact on 5G mmWave Mobile Devices

AHMAD ALAMMOURI[1], (Student Member, IEEE), JIANHUA MO[2], (Member, IEEE), BOON LOONG NG[2], (Member, IEEE), JIANZHONG CHARLIE ZHANG[2], (Fellow, IEEE), AND JEFFREY G. ANDREWS[1], (Fellow, IEEE)

[1]Wireless Networking and Communications Group (WNCG), The University of Texas at Austin, Austin, TX 78712, USA
[2]Standards and Mobility Innovation Lab, Samsung Research America, Richardson, TX 75082, USA

Corresponding author: Ahmad Alammouri (alammouri@utexas.edu)

ABSTRACT This paper contributes a comprehensive study on the effect of the user hand grip on the design of 5G millimeter-wave (mmWave) mobile handsets, specifically in terms of the antenna module placement and the beamforming codebook. The high-frequency structure simulator (HFSS) is used to characterize the radiation fields for different antenna placements and 14 possible handgrip profiles based on the experiments that we conducted. The loss from hand blockage on the antenna gains can be up to 20–25 dB, which implies that the possible hand grip profiles need to be taken into account while designing the antenna module placement and beamforming codebook. Specifically, we consider three different codebook adaption schemes: a grip-aware scheme, where perfect knowledge of the hand grip is available; a semi-aware scheme, where just the application (voice call, messaging, and so on) and the orientation of the mobile handset is known; and a grip-agnostic scheme, where the codebook ignores the hand blockage. Our results show that the ideal grip-aware scheme can provide more than 50% gain in terms of the spherical coverage over the agnostic scheme, depending on the grip and orientation. Encouragingly, the more practical semi-aware scheme that we propose provides performance approaching the fully grip-aware scheme. Overall, we demonstrate that the 5G mmWave handsets are different from pre-5G handsets: the user grip needs to be explicitly factored into the antenna placement and the codebook design.

INDEX TERMS 5G mobile phone, beamforming, codebook design, hand blockage, hand grips, mmWave.

I. INTRODUCTION

With the release of the first phase of the fifth-generation (5G) cellular standard and the availability of several millimeter-wave (mmWave) bands [1] for commercial use, the push now is on providing commercial mobile devices that are capable of operating on the mmWave bands and harvesting the promised high data rate gains. However, before this step, some aspects of mmWave communications have to be considered from a more practical perspective.

A critical aspect that is typically overlooked in previous studies is the design of the mobile device. Designing the antennas for mmWave mobile devices along with their placement is a challenging task due to the multiple trade-offs that have to be taken care of by the designer. For example, multiple antennas are required to have a reasonable array gain and harvest the promised benefits from mmWave communications. In addition, due to self-attenuation and reflections of the device and the sub-hemispherical coverage of the patch antennas [2], different arrays with different locations and orientations are also required to be able to receive signals from different directions, such that each array is responsible for receiving signals over a particular set of directions, referred to as the coverage region. Although this is required for any device that uses mmWave including base stations (BSs) and access points, the problem is more challenging and critical for mobile devices since the user cannot be forced to hold to phone in certain orientation and due to mobility, the signal could possibly arrive from any direction without restrictions.

Moreover, due to the sensitivity of mmWave to blockage by the human hands [3] and the need for RF compliance rules as required by the FCC for safety purpose [4], [5], the designer has to account for the possible hand blockage in the antenna placement and design. In other words, there must be overlap between the coverage regions of each antenna array, such that if an array is blocked, the mobile device has coverage through other arrays.

The associate editor coordinating the review of this manuscript and approving it for publication was Ning Zhang.

A. MOTIVATION AND RELATED WORK

In practice, there are many limitations on the number of antennas per array and the number of arrays due to form factor, power, and complexity constraints. Note that due to the self-attenuation of the device caused by the screen, the battery, and the metallic frames, the arrays have to be placed on the exterior of the device [2], which means that they will compete for space with other modules of the phone, such as the camera, the speaker, the microphone, buttons, etc. Furthermore, more antennas and more antenna arrays escalate the power consumption and the complexity of beam management in terms of beam training, tracking, and switching.

Another aspect that is highly affected by the hand blockage is the beam codebook design. Beamforming, which is required to combine the signals from different antennas, is a critical part of mmWave communications since it relies on high array gains [6]. Although digital beamforming is elegant theoretically and results in excellent array gains, the commercial devices will most probably avoid using fully-digital beamforming due to its complexity, both in hardware and signal processing [7], [8]. Instead, analog beamforming, which is based on pre-designed codebooks, is proposed as an alternative and supported by the 3GPP standard [9]. The idea behind it is that the designer priorly determines a set of beamforming vectors (codewords), and the device switches between these codewords to select the one that maximizes the antenna gain in the direction of the received signal. A comparison between digital and analog codebook beamforming has been conducted recently in [9], where the authors showed that the codebook beamforming can balance the trade-off between the overhead complexity and array gain and can perform close to the digital beamforming. Another interesting study was performed in [8], which proposes and compares different heuristic approaches to design the beam codebooks taking into account the antennas' radiation pattern.

However, [8] only considers the free space propagation without the possible hand blockage and [9] focuses on comparing different antenna types and comparing the analog codebook beamforming and the digital one. Moreover, their model of the human hand is either based on a stochastic model [10], which assumes a 30 dB flat loss in the antenna gain due to the hand blockage, or a statistical loss [3], which only differentiates between the blockage in landscape and portrait orientations. It is well-known that users hold their phones in different ways depending on the applications they are using, the environment, and their habits. These different hand grips affect the radiation patterns in distinct ways even though the phone orientation is the same. For example, while in the landscape orientation, the user can hold the phone with both hands or a single hand while watching a video or taking a picture. The effect of the single hand blockage on the radiation patterns can be quite different from that of dual hand blockage because when the finger is near the antenna, the radiation is influenced more by coupling, reflection, and attenuation caused by the finger [11], [12].

B. SUMMARY OF CONTRIBUTION

The contribution of this work is to provide a comprehensive study on the impact of the user hand grip on the performance of the mobile device as a complementary to the recent studies in [8], [9] and discuss how the designer can account for the user hand grip. We consider two different practical designs for the mobile device in terms of the antenna arrays placement that are based on proposals in 3GPP meetings [13]–[15]. To capture the antenna radiation patterns, we use an electromagnetic simulation software called high-frequency structure simulator (HFSS) [16]. To avoid using over-simplified analytical models, we also include our model of the human hand into the simulations to capture the irregularities in the radiation patterns caused by the hand. Furthermore, we discuss a simplified way to construct the antenna radiation pattern for any hand grip without the need to simulate the whole setup again using HFSS. Moreover, due to unavailability of public data sets on how users hold their phone in terms of the positions of their fingers, we conduct our own experiment, where we asked users to hold their phones and perform certain activities to get an idea on the common hand grips for each activity.

First, we compare the two mobile designs assuming free space propagation and blockage by human hand, and we show that the design has to account for the possible blockage by the human hand. Otherwise, a significant loss in the antenna gain will occur which risks the user's connectivity. Moreover, we show that the analog beam codebook design is also sensitive to the hand blockage. To this end, we compare three different schemes of beam codebook adaptation, where the codebook is updated based on some knowledge about the user hand grip: An idealistic *grip-aware* scheme, which assumes that the device can accurately detect the hand grip and use a codebook that is specifically designed for it; a more practical scheme we call the *semi-aware* scheme, which is based on the assumption that the device only knows the orientation of the device and the active application the user is using; and a benchmark *grip-agnostic* scheme, where the codebook is designed assuming no-blockage and is not adapted according to the hand grip. We show that the *grip-aware* and the *semi-aware* schemes can achieve over 57% gain in terms of the spherical coverage compared to the *grip-agnostic* scheme, where the gain depends on the activity.

C. PAPER ORGANIZATION

The rest of the paper is organized as follows: In Section II, we discuss the models we adopted for the antenna arrays, mobile device, and human hand in addition to the algorithms used to design the beam codebook. We also discuss a simplified way to simulate different hand grips. In Section III, we discuss the findings of our own experiments on the different hand grips seen while performing different activities on the phone. Section IV is focused on the different schemes that account for the hand grip in the beam codebook design.

TABLE 1. Notation.

Notation	Definition	Default Value
N_p	The number of sampling points on the unit sphere.	5809
N_t	The number of antennas on the mobile phone.	16 or 24
N_c	The codebook size.	8
N_d	The size of the candidate set of codewords.	363
$\mathbf{w}$	A codeword which represents the complex weights on each antenna.	–
$\mathcal{W}_c$	The final codebook.	–
$\mathcal{W}_d$	The set of candidate codewords.	–
$\mathcal{X}$	The set of all points on the unit sphere which also represents the set of all possible directions.	–
θ	The elevation angle.	$0^\circ \leq \theta \leq 180^\circ$
ϕ	The azimuth angle.	$0^\circ \leq \phi < 360^\circ$
$G_i(\mathbf{w})$	The gain at the i^{th} point given a codeword $\mathbf{w}$.	–
$\mathbf{M}_i$	The antennas response at the i^{th} point.	–

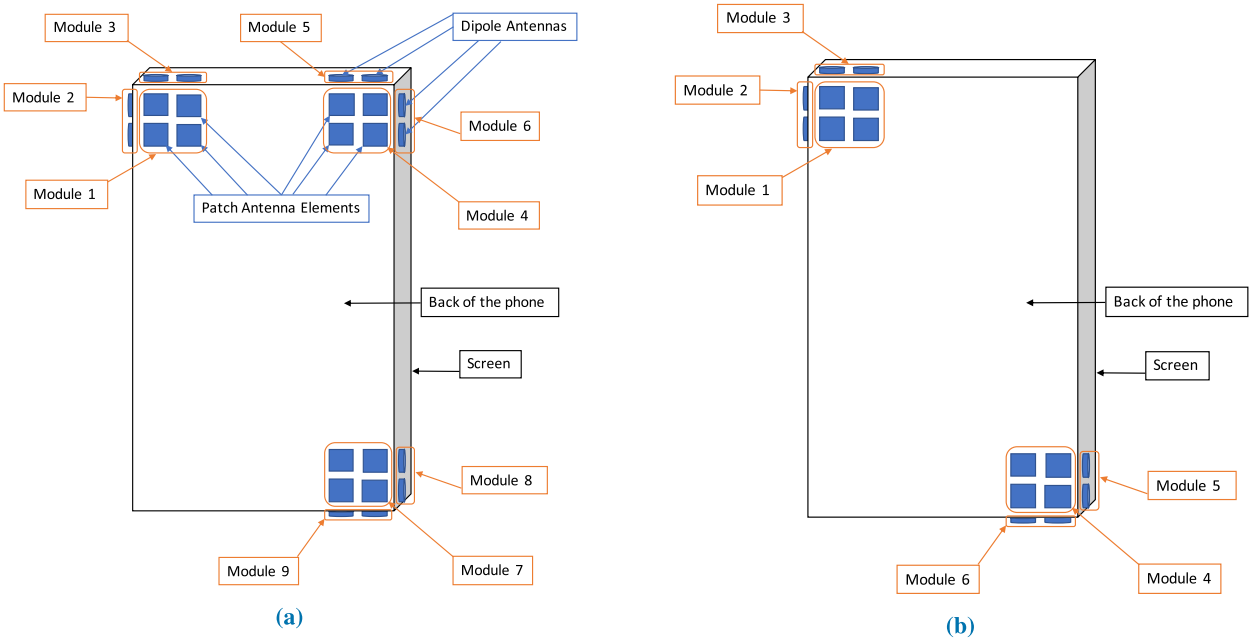

FIGURE 1. The considered antenna placements. (a) Design 1. (b) Design 2.

The main results are presented in Section V before the conclusion in Section VI.

II. SYSTEM MODEL

To show the effects of the hand grip on the antennas' radiation patterns and the beam codebook design, we must first have a model for the antenna arrays, their placement in the mobile phone, and of the human hand. This section discusses and justifies these models. We also briefly discuss the adopted algorithms in designing the beam codebooks. The notation used throughout this paper is summarized in Table 1.

A. ANTENNA AND MOBILE DESIGN

As we mentioned earlier, a good design for the mobile device must have different antenna arrays with different orientations, such that each array is able to receive the signal from certain directions (coverage region). What's more, there must be overlap between the different coverage regions for the antenna arrays to account for possible hand blockage. To this end, different antenna designs were proposed in 3GPP meetings [13]–[15] and studied in the literature [2], [9], [17] to ensure the previous requirements. The main types of antenna arrays in these designs are the patch antenna array and dipole antenna array. The 2-D patch arrays are typically placed on the back (face) of the phone, due to the width constraint on the edges of the phone, and dipole arrays are placed on the edges of the phone. With 1-D patch array, it may be possible to place the arrays on the edges of the phone, however we do not consider such configuration here and the conclusions are not expected to be affected by this. Inspired by these designs, we consider the following two designs in this work:

Design 1: In this design, we have three 2×2 patch antenna modules placed on top two corners and the right bottom corner of the back of the phone. Also, each is surrounded by two modules of dipole antennas on the edges. This design is shown in Fig. 1a.

Design 2: In this design, we have two 2×2 patch antenna modules placed on opposite corners of the back of the phone. Each is also surrounded by two modules of dipole antennas on the edges. This design is shown in Fig. 1b.

Note that both designs consider a mix of edge (dipole) and face (patch) antenna arrays. This is because the 2×2 patch array provides good spherical coverage to the hemisphere on the back of the phone, but it cannot be used to receive (transmit) signals from (through) the front end of the phone because of the front-to-back ratio of the patch antenna as well as the blockage of the screen [3]. On the other hand, the dipole antenna arrays can be used to extend the coverage region to the sides of the device, but it also restricts us to linear antenna arrays due to size constraints. Hence, a good design should consider both of these antenna types to provide good spherical coverage. Note that there is also redundancy since some arrays point to the same direction. This is because we need to account for possible hand blockages which can severely reduce the gain of the blocked antenna as shown later in this work. Note other works in the literature refer to the patch array along with its two adjacent dipole arrays as a single module. In this work, we call each one of the arrays a module.

To reduce the complexity of the management and design of the beam codebook, the mobile device is restricted to use one array at a time, referred to as an antenna module, which is either a 2×2 patch array or a 1×2 dipole array. Hence, in total, we have 6 modules in Design 2, two 2×2 arrays and four dipole antenna modules, and 9 modules in Design 1, three 2×2 patch arrays and six dipole antenna modules. These designs will be studied and compared in the following sections in terms of the spherical coverage in free space as well as in the presence of the hand blockage. In the next section, we formally define the spherical coverage and the problem of designing beam codebooks.

B. SPHERICAL COVERAGE AND HFSS

The main performance metric considered in this work is the spherical coverage which corresponds to the antennas' far field gain over all possible directions. To quantify it, we discretize the unit sphere uniformly, and then the antenna gain is found for each point on the sphere. More rigorously, let $\mathcal{X} = \{x_i = (\theta_i, \phi_i),\ \forall i \in \{1, 2, \cdots, N_p\}\}$ be a set of points uniformly distributed on the surface of the unit sphere, where N_p is the number of points[1] and $0^\circ \leq \theta_i \leq 180^\circ$, $0^\circ \leq \phi_i < 360^\circ$ are the spherical coordinates of the i^{th} point. Each point represents one possible direction for the signal to arrive from. In other words, we have discretized the possible angle of arrivals (AoAs). One way to obtain such a set is through Fibonacci grids [18] which give a set of points that are approximately uniformly placed on the sphere. An illustration is shown in Fig. 2.

[1]The number of sampling points needed depends on the *smoothness* of the radiation pattern. More irregularities in the radiation pattern means more sampling points are needed to have an accurate estimation of the spherical coverage.

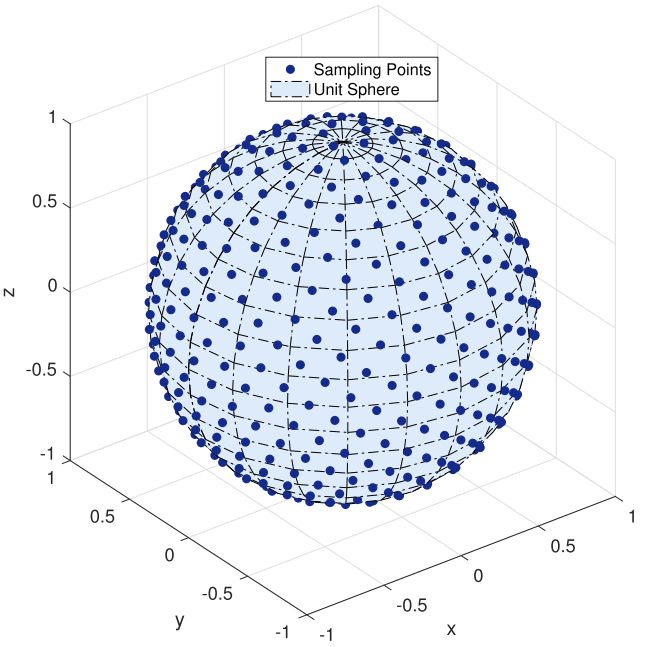

FIGURE 2. A uniform sampling of the unit sphere using Fibonacci grids with $N_p = 501$.

Let the gain at point x_i be denoted by $G_i(\mathbf{w}) \in \mathbb{R}_+$, given a beamforming vector $\mathbf{w} \in \mathbb{C}^{N_t \times 1}$, where N_t is the total number of antennas[2]. Then the spherical coverage is defined by the set of gains over all the points on the sphere:

$$\mathcal{S}(\mathbf{w}) = \{G_i(\mathbf{w}),\ \forall i \in \{1, 2, \cdots, N_p\}\}. \tag{1}$$

We will focus on the whole distribution of the set $\mathcal{S}(\cdot)$, since the signal can arrive from any direction to the mobile phone. More specifically, we focus on the 20^{th}, 50^{th}, and 80^{th} percentiles in addition to the mean.

To compute the antenna gain $G_i(\mathbf{w})$ given a certain setup of antennas, we use an electromagnetic simulation software called HFSS [16] since the theoretical models fall short in capturing the irregularities in the antennas' radiation patterns. Both of the designs of the mobile phone discussed in the previous section were built in HFSS. The antennas were designed for 39 GHz carrier frequency with a half wavelength separation. In these designs, we did not add the different components in the phone and only modeled the screen, since it is the main source of reflections and absorption.[3]

Using HFSS, we get the antenna response of each element in each array for each direction x_i. Hence, for a given direction x_i, we have an antenna response vector which we denote by $\mathbf{M}_i \in \mathbb{C}^{1 \times N_t}$. Hence, for a given beamforming vector $\mathbf{w}$, the antenna gain $G_i(\mathbf{w})$ is given by

$$G_i(\mathbf{w}) = \mathbf{w}^H \mathbf{M}_i^H \mathbf{M}_i \mathbf{w}, \tag{2}$$

[2]Note that since we assumed only one antenna module can be active at any time, the vector $\mathbf{w}$ has few non-zero elements.

[3]Other modules in the phone can cause $1 - 2$ dB loss in gain [2], but it varies depending on the design of the phone, and there is no standard structure for that.

where $\mathbf{w}^H$ is the Hermitian or the conjugate transpose of the vector $\mathbf{w}$. Note that equation assumes a single polarization; horizontal or vertical. For more details on how to get the response $\mathbf{M}_i$ from HFSS and how to account for dual polarization, refer to [8].

At this point, we need to choose a set of beamforming vectors to maximize some function of the spherical coverage. The set of beamforming vectors is denoted by $\mathcal{W}_c$ and referred to by a codebook hereafter, where each beamforming vector is called a codeword. To this end, we focus on two approaches to design the codebook; one approach provides a theoretical upper bound on the spherical coverage, and the other takes into account practical constraints on the codebook design.

- **Upper Bound**: A codeword is picked for each point x_i to maximize the gain at this point. Hence, the codebook has the same size as the considered number of sampling points on the sphere, N_p, which is very large. Moreover, it is based on the assumption that the phases of the weights in the codewords can have any arbitrary value without discretization which is not true in practice.
- **Practical Design**: A limited codebook size with per-antenna power constraint and a finite set of possible phase values. It takes into account the complexity of beam management (beam switching and tracking) in terms of the codebook size and the practical power amplifier and phase shifters which are typically fed by a few bits.

For the upper bound, we choose the codeword that maximizes the gain for each point x_i. Based on (II-B), the maximizer is the eigenvector that corresponds to the maximum eigenvalue of $\mathbf{M}_i^H \mathbf{M}_i$. For the practical design, we design a codebook $\mathcal{W}_c$ that has N_c codewords which have to satisfy a constraint on the number of bits of the phase shifters. Note that the definition of the spherical coverage in (1) is for a given codeword $\mathbf{w}$. However, given a set of codewords (a codebook), the spherical coverage is defined as follows

$$\mathcal{S}(\mathcal{W}_c) = \{ \max_{\mathbf{w}\in\mathcal{W}_c} G_i(\mathbf{w}),\ \forall i \in \{1, 2, \cdots, N_p\}\}, \tag{3}$$

which means that for each point x_i, we search for the maximum possible gain obtained from all the codewords in the codebook $\mathcal{W}_c$. Based on this, the mean spherical coverage across all points on the sphere given a codebook $\mathcal{W}_c$, denoted by $\bar{\mathcal{S}}(\mathcal{W}_c)$, is given by

$$\bar{\mathcal{S}}(\mathcal{W}_c) = \frac{1}{N_p} \sum_{i=1}^{N_p} \max_{\mathbf{w}\in\mathcal{W}_c} G_i(\mathbf{w}). \tag{4}$$

In this work, we choose the codebook $\mathcal{W}_c$ that maximizes the mean spherical coverage out of a given large set of candidate codewords $\mathcal{W}_d$, where the set $\mathcal{W}_d$ satisfies all the required conditions on the maximum transmit power and the finite number of bits in the phase shifter. Hence, we have the following optimization problem.

$$\mathcal{W}_c = \underset{\mathbf{w}_1,\cdots,\mathbf{w}_{N_c}\in\mathcal{W}_d}{\arg\max}\ \bar{\mathcal{S}}(\{\mathbf{w}_1, \cdots, \mathbf{w}_{N_c}\}). \tag{5}$$

which is a combinatorial problem and solving it using exhaustive search which is not feasible given a large set $\mathcal{W}_d$ and a large number of points N_p. Different heuristic approaches to solve this problem were discussed in details in [8]. In this work, we adopt the greedy approach which we briefly describe in the following for completeness. The greedy approach is an iterative one, where the first codeword is selected to maximize the mean spherical coverage

$$\mathbf{w}_1 = \underset{\mathbf{w}\in\mathcal{W}_d}{\arg\max} \frac{1}{N_p} \sum_{i=1}^{N_p} G_i(\mathbf{w}). \tag{6}$$

The second codeword is chosen to maximize the mean spherical coverage, given that $\mathbf{w}_1$ was already chosen. Hence, the second codeword is chosen such that the mean spherical coverage formed by the composite gain of the chosen codeword and $\mathbf{w}_1$ is maximized. Mathematically,

$$\mathbf{w}_2 = \underset{\mathbf{w}\in\mathcal{W}_d\setminus\mathbf{w}_1}{\arg\max} \frac{1}{N_p} \sum_{i=1}^{N_p} \max\left(G_i(\mathbf{w}), G_i(\mathbf{w}_1)\right). \tag{7}$$

Intuitively, the second codeword will point the beam in a different direction than the first codeword to cover a larger region which maximizes the mean coverage. Subsequently, the N^{th} codeword is found by

$$\mathbf{w}_N = \underset{\mathbf{w}\in\mathcal{W}_d\setminus\{\mathbf{w}_1,\cdots,\mathbf{w}_{N-1}\}}{\arg\max} f(\mathbf{w}),$$
$$f(\mathbf{w}) = \frac{1}{N_p} \sum_{i=1}^{N_p} \max\left(G_i(\mathbf{w}), G_i(\mathbf{w}_1), \cdots, G_i(\mathbf{w}_{N-1})\right). \tag{8}$$

This approach is only optimal if the desired codebook size is one and otherwise, it is suboptimal. However, it was shown in [8] that it performs comparably good to other more sophisticated algorithms and it approaches the previously mentioned upper bound for large codebook size. Before wrapping up this section, we discuss the choice of the candidate set of codewords $\mathcal{W}_d$. There are many options to choose from as shown in [8]. In this work, $\mathcal{W}_d$ is generated by following the same approach we used to find the upper bound. More specifically, we select a subset of points $\mathcal{Y}$ from $\mathcal{X}$ (i.e., $\mathcal{Y} \subset \mathcal{X}$) that has a length $N_d \ll N_p$. Then, for each point $y \in \mathcal{Y}$, we select the codeword that maximizes the antenna gain at this point by eigenvalue decomposition. Finally, the phases of the codewords are quantized according to the number of bits of the phase shifters N_b. Hence, $\mathcal{W}_d$ is a subset of the codewords we use to evaluate the upper bound, but with discrete phases. Note that the choice of $\mathcal{W}_d$ is not very critical as shown in [8] as long as N_d is big enough.

Based on what we presented so far, we can design codebooks for the mobile designs we mentioned before and evaluate the performance compared to the upper bound assuming free space propagation. However, our focus in this work is on the effect of hand blockage on the antenna radiation pattern and the codebook design. To this end, we discuss the hand model in the next section and show how different hand grips can be included in our HFSS simulations.

C. HAND MODEL

There are several works in the literature that study the effect of the hand blockage on the antennas' radiation patterns in mmWave bands [3], [11], [12], [19]. The results are based on measurements or sophisticated simulations, and they all agree that the hand blockage can have detrimental effects on the radiation patterns. For quantitative and analytical models, the 3GPP standard [10] assumes a 30 dB loss across a region on the sphere around the cell phone, where the boundaries of this region depend on whether the phone is held in landscape or portrait. This model was revisited in [3], where a statistical model for the affected region was proposed instead of a flat 30 dB loss. However, both of these models do not differentiate between different hand grips and only distinguish the portrait and the landscape orientations of the phone.

As we mentioned earlier, it is well-known that users hold their phones in different ways depending on the applications they are using, the environment, and their habits. These different hand grips affect the radiation patterns in distinct ways although the phone orientation is the same. For example, while in the landscape, the user can hold the phone with both hands or a single hand while watching a video or taking a picture. The effect of the single hand blockage on the radiation patterns can be quite different from that of dual hand blockage because when the finger is near the antenna, the radiation is influenced more by coupling, refection, and attenuation caused by the finger [11], [12]. Particularly, when the finger is close to the antenna, it can cause an impedance mismatch which can lead to a noticeable drop in the antenna gain [20].

Moreover, since we have arrays of antennas, the finger can cause a gain imbalance between the different elements of the array and can reduce the diversity between them [21]. Hence, although the analytical models provide a good tool to quantify the loss due to hand blockage, they cannot be used in our case since we need to study the effects of different hand grips on the radiation patterns. Our approach is to model the human finger and then include it into HFSS simulations which will take care of all the possible irregular effects of the hand on the antenna radiation pattern.

Different models for the human hand were used in the literature, from a real hand model to cylinders and bricks models, where, as the names imply, the fingers are either modeled as cylinder or brick [22], [23]. For the material inside, one can construct an non-homogeneous model where the skin, the muscles, the fat, and the bones are represented by different layers each with its own dielectric properties. On the other hand, in homogeneous models, the dielectric properties are averaged over the different materials of the human finger. It was shown before that a homogeneous cylinder or brick model provides sufficient accuracy for the loss in sub-6 GHz [22]. However, in high frequencies like in mmWave band, the skin plays the major part in reflection and absorption. Hence, some previous works only consider the skin [3]. In our work, we consider a two-layer model as in Fig. 3, where

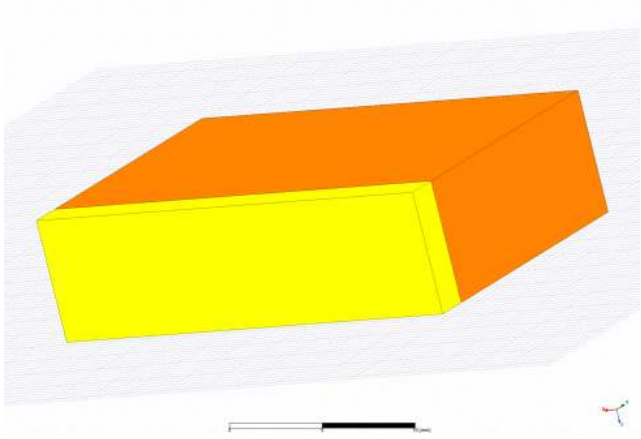

FIGURE 3. Our model for the human finger in HFSS, where the yellow layer is the skin and the orange is the rest of the finger.

TABLE 2. Dielectric properties of different materials at frequency 39 GHz.

Material	Conductivity [S/m]	Relative permittivity	Loss tangent
Skin (Dry)	31.429	11.983	1.2089
Skin (Wet)	32.432	14.386	1.0391
Muscle	42.501	18.639	1.051
Fat	2.174	3.424	0.2926
Bone	6.28	4.7268	0.5637
Layer 1	31.9305	13.1845	1.124
Layer 2	12.703	7.248	0.6069

the first corresponds to the skin and the second models the rest of the human finger. The dielectric properties for the skin are averaged over the wet and dry conditions and the dielectric properties for the second layer are averaged over the properties of the bone, muscle, and fat. The used values are shown in Table 1 and taken from [24]. The size of the finger is taken to be the average size of personnel in the US Army as recorded in [25] and the thickness of the skin is assumed to be 2 mm [11].

Given this model for the hand, we can show the effect of the hand blockage on the antenna's radiation pattern. In Fig. 4 we plot the spherical antenna gain of one of the patch antenna element we designed with and without blockage, where these results are directly taken from HFSS simulations. The figure shows about 20-25 dB loss in the boresight direction (z-axis). It also shows the irregular effect of the blockage on the radiation pattern which makes it hard to predict using an analytical model and justifies our reliance on HFSS simulations to capture the effect of reflections, couplings, and attenuation caused by fingers. Note that this loss does not depend on the codebook design and it is purely based on the blockage of a single patch antenna element. Hence, it is still not clear at this point how the blockage due to the whole hand grip will affect the spherical coverage, which is our main performance metric, especially that some antennas may not be blocked assuming specific grips. For this, we discuss first how to simulate various hand grips in the next section.

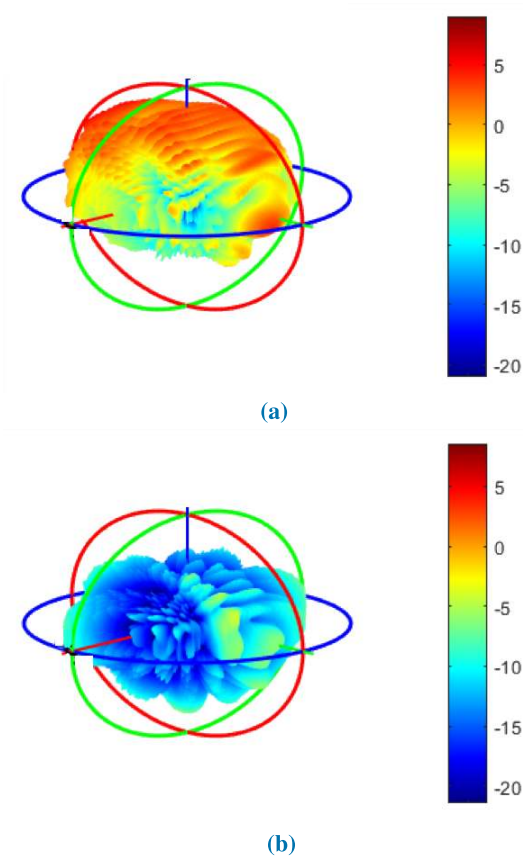

FIGURE 4. The 3D antenna gain in dB of a patch antenna with and without the blockage by a finger. (a) Without blockage. (b) With blockage.

D. SIMULATING DIFFERENT HAND GRIPS

Due to the diverse hand grips in terms of the position of the fingers on the phone, simulating all of them, where we take precisely the positions of the fingers on the phone, is infeasible. Hence, we consider a simplified way where we partition the faces of the phone into disjoint regions, each with the size of the antenna module. We focus on the cases where the region is fully blocked. In other words, in case of blocking, we assume that the finger covers the whole region. This is a reasonable assumption given that the antenna modules are small compared to the finger due to the short wavelength.

Moreover, since the loss is more severe when the fingers are in close proximity to the antenna, due to the reflections, coupling, and possible gain imbalance and impedance mismatch as we mentioned earlier, we focus on the regions at the corners of the mobile phone as shown in Fig. 5, where the antenna modules are placed. Note that in total, we have 16 possible regions at the corners of the mobile phone. However, four of those are located on the screen. The radiation through these four regions suffers a huge attenuation from the screen in addition to the front-to-back loss of the patch antennas as shown in Fig. 4a which shows about 25 dB difference in the gain between the boresight (z-axis) and through the screen (negative z-axis). Hence, we neglect the blockage in these

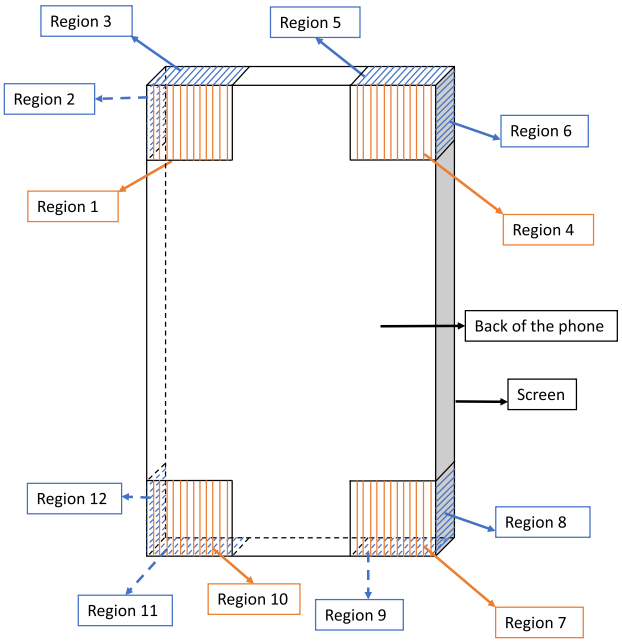

FIGURE 5. The considered regions for hand blockage.

regions which leaves us with 12 different regions as shown in Fig. 5.

Based on this, we have 2^{12} possible combinations of blocked regions. Simulating all of these is infeasible since simulators like HFSS are time-consuming. Consequently, we simulate the 12 cases which correspond to the presence of the finger on each region separately; these cases are referred to as the elementary cases hereafter. For each elementary case, we have an antenna response vector for each point x_i, $\mathbf{M}_i^{(j)}$, where $j \in \{1, 2, \cdots, 12\}$, which we get from HFSS. Then for the cases where more than one region is blocked, we construct the radiation pattern using the elementary cases as follows.

Assume that for a certain grip n, the blocked regions are given by the set $\mathcal{B} \subset \{1, 2, \cdots, 12\}$ and the antenna response vector for this grip at point x_i is denoted as $\mathbf{M}_i^{(n)}$. Then the response for the m^{th} antenna is given by

$$\mathbf{M}_i^{(n)}(m) = \mathbf{M}_i^{(j^*)}(m), \tag{9}$$

where

$$j^* = \underset{j \in \mathcal{B}}{arg\,min}\ |\mathbf{M}_i^{(j)}(m)|, \tag{10}$$

which means that for each antenna and each point x_i, the antenna response is chosen to be the one that has the minimum gain from all the responses of the cases given in $\mathcal{B}$. An illustration is given in Fig. 6, where the objective is to find the antenna response of the scenario on the right side given the radiation pattern of the two elementary cases on the left side. By following this approach, we can find the radiation pattern given any hand grip using just the 12 elementary cases we discussed, which significantly simplifies finding the

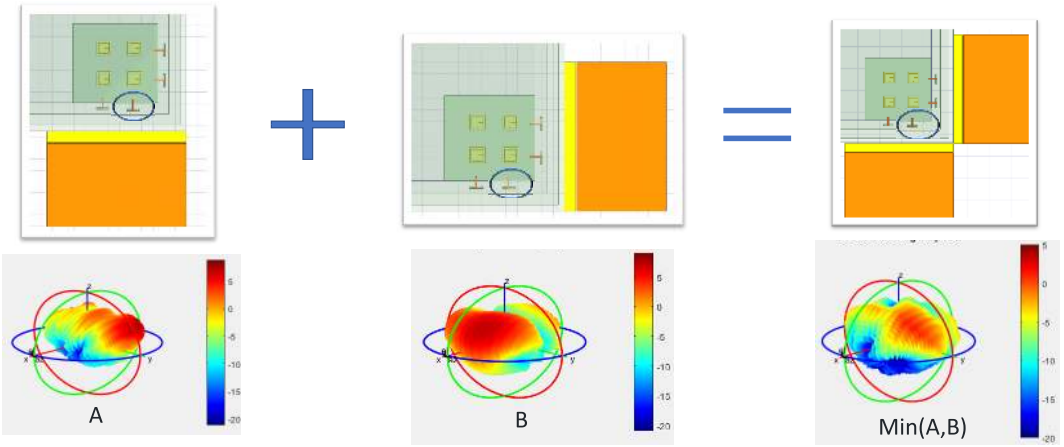

FIGURE 6. Constructing the antenna response of the circled antenna element from the elementary cases, where the orange and yellow object is the finger.

TABLE 3. Different hand grips along with the blocked regions.

Grip ID	Blocked Regions
1	None
2	1, 3, 4, 5, 7,9.
3	7, 8, 9.
4	7, 8.
5	8.
6	1, 2, 3, 4, 5, 7, 9.
7	1, 2, 3, 4, 5, 7, 8, 9.
8	1, 2, 3, 5, 7, 9.
9	4, 7, 8, 9.
10	1, 2, 3, 4, 5, 7.
11	1, 2, 3, 5, 6, 7, 8, 9.
12	2, 3, 4, 5, 6.
13	1, 2, 3.
14	1, 4, 7.

radiation patterns, since it can be found without the need of using HFSS. In the next section, we present the results of our own experiments on the different possible hand grips.

III. ACTIVITIES AND HAND GRIPS

Up to our knowledge, there are no available database that record how users hold their phones while performing certain activities[4]. Hence, we performed our own experiment. We asked eight users to hold a phone and perform certain activities and then the blocked regions, shown in Fig. 5, were noted by covering the phone with stickers similar to Fig. 5. Since the antennas in our designs are placed on the regions $1-9$, we focus on these regions. The users were asked to watch a video, play a game, make a phone call, and text a message in both landscape and portrait orientations. The obtained hand grips are summarized in Table 3, where we list the blocked regions for each grip. For comparison, we include the no-blockage case and denote it as Grip 1. In Table 4, we show the type of grids observed for each activity along with their frequencies. In addition, we have included the case where the phone is in the user's pocket and the screen is facing outwards for comparisons. These results will help us in the next sections in correlating the hand grips with certain activities.

[4]In [26], it was recorded how people hold their phones while performing certain activities, but it did not actually show the placement of the fingers on the device.

TABLE 4. Activities and hand grips.

Activity	Grip IDs	Respective Probabilities
Game Portrait	3	1
Game Landscape	6, 7 ,8	$3/8$, $2/8$, $3/8$.
Video Portrait	4, 9, 12	$3/4$, $1/8$, $1/8$.
Video Landscape	3, 10, 11, 12	$1/8$, $3/8$, $1/4$, $1/4$.
Messaging Portrait	3	1
Messaging Landscape	2, 6, 13	$3/8$, $1/4$, $3/8$
Voice Call	3, 4, 5	$1/4$, $1/2$, $1/4$
Pocket	14	1

IV. CODEBOOK ADAPTATION WITH HAND GRIPS

Using HFSS along with our models for the mobile phone and the hand, we can obtain the antenna gains for each grip in Table 3. This section focuses on how the codebook design can be influenced by these grips. We focus on three schemes: a *grip-aware* scheme which assumes that the mobile phone has a full knowledge of the current user grip, and a *semi-aware* scheme which only assumes the knowledge of the application the user is using and the orientation of the phone, and a *grip-agnostic* scheme which assumes that the codebooks are designed assuming no blockage, and they are not altered based on the hand grip.

A. GRIP-AWARE SCHEME

For this scheme, we assume that the phone knows exactly the hand grip and the corresponding antenna radiation patterns. With this knowledge, the phone determines a codebook that is specifically optimized for the current user grip. Although estimating the user hand grip by the mobile phone, through capacitive touch sensors and infrared proximity

sensors [27], [28], can bring many benefits in terms of providing a natural experience between the mobile phone and the user, current devices do not have the capabilities to provide an accurate estimation of the user hand grip. Moreover, it requires a different codebook for each different grip which may not be feasible due to storage limitation in the RF chipset and the switching overhead. Accordingly, this scheme can be thought of as an upper bound on the gain we can achieve by adapting the codebook based on the user grip. The codebook design algorithm in this scheme is the same as designing the codebook for the free space case described in Section II-B, except that the antenna response vectors $\mathbf{M}_i,\ \forall i \in \{1, \cdots N_p\}$ are replaced by the antenna response vectors for each grip which are found by using the methods we described in Section II-D.

B. SEMI-AWARE SCHEME

In this scheme, only the orientation of the phone and the application the user is operating are assumed to be known by the mobile device. The rationale behind it is that although users hold their phones in various ways while performing the same activity depending on their personal habits and the environment, there are certain patterns that are highly correlated for a given activity. An analogy was drawn in [28] with traditional hand tools (e.g., hammer, cup, etc.), where the grip can be different for individual users, but still there is a correlation between different grips.[5] Hence, in this scheme, we exploit this correlation by designing a codebook for each activity, instead of a codebook for each hand grip, which significantly reduces the number of stored codebooks. Moreover, current mobile phones can distinguish the orientation of the phone along with the application the user is using (or at least the genre of the activity). Therefore, this is practical, unlike the Grip-Aware Scheme.

The codebooks are designed as follows: for each pair of activity and orientation, design a codebook that maximizes the weighted mean of the spherical coverage over the common hand grips for this activity and orientation. We choose the *weighted* mean since some grips are less common than others. However, the weighted mean is just an example of the desired objective function. The same algorithm can be used to maximize the minimum over all the grips (i.e., the design is based on the worst case scenario) or the sum-log of the spherical coverage, to ensure some fairness across different grips.

Mathematically, denote the set of grips for an activity as $\mathcal{B}$ and the corresponding likelihood matrix as $\mathbf{P}$. Then the codebook is found by solving the following optimization problem, which is an extension to (5).

$$\mathcal{W}_c = \underset{\mathbf{w}_1,\cdots,\mathbf{w}_{N_c}\in\mathcal{W}_d}{\arg\max} \sum_{j\in\mathcal{B}} \mathbf{P}(j)\bar{\mathcal{S}}^{(j)}(\{\mathbf{w}_1, \cdots, \mathbf{w}_{N_c}\}), \quad (11)$$

[5]Note that in our work, we try to estimate the grip based on the activity and the orientation. In [28], it is the opposite, i.e., they tried to estimate the activity based on the grip.

where $\bar{\mathcal{S}}^{(j)}(\cdot)$ is the average spherical gain, as defined in (4), for the j^{th} grip. In the next section, we use our own data regarding the different grips in Table 3 and the different activities in Table 4 to evaluate the performance of this scheme.

C. GRIP-AGNOSTIC SCHEME

This is the benchmark scheme, where the codebook is designed assuming no blockage, and the mobile phone does not adapt its codebook with different hand grips. Hence, the codebook is designed exactly as described in Section II-B.

In the next section, we compare these schemes, and show the importance of including the hand grips into the beam codebook design.

V. SIMULATION RESULTS

In this section, we study the performance of the different mobile designs in Fig. 1 and the different schemes discussed in Section IV in terms of the spherical coverage. The raw radiation data is taken from HFSS and processed in MATLAB where we implement the different algorithms and schemes discussed throughout this work. The default values of the different parameters are taken as in Table 1 with the exception that we focus on the spherical coverage over the region described by $0° \leq \theta \leq 100°$ and $0° \leq \phi < 360°$, where θ is the elevation angle, and ϕ is the azimuth angle, which includes the whole hemisphere facing the back of the phone, plus the adjacent 10 degrees from the other hemisphere. The reason behind this choice is that the region directly facing the screen is already dead because of the screen blockage and the front-to-back attenuation of the patch antennas as we described earlier. Hence, changing the codebook design algorithms or the hand grip schemes will not have an impact on this region.

A. DIFFERENT DESIGNS OF MOBILE DEVICE

We start by comparing the spherical coverage of the two designs illustrated in Fig. 1 assuming no hand blockage. The CDF of the spherical coverage of the two designs is shown in Fig. 7, where both the upper bound (infinite codebook size) and the practical codebook design (limited codebook size) are plotted. First, note that there is a gap between the upper bound and the practical codebook with 15 codewords. This gap is due to the huge difference between the codebook sizes, enforcing the equal power allocation across the antennas and limiting the phase shfiter's bits to 5. Nonetheless, this gap is less than one dB in terms of the 50^{th} percentile, which shows the effectiveness of the greedy algorithm that is used to design the codebook, and the gap can be further reduced by increasing the codebook size. Note also that the quantization of the phases of the codewords, due to the limited number of bits fed to the phase shifters, adds to this gap. But it was shown in [8] that having 5 bits is sufficient to recover most of the loss due to phase quantization.

The second observation from Fig. 7 is that the performance of the two mobile designs is very close: less than 2% gap for the 50^{th} percentile. This minor enhancement in the spherical

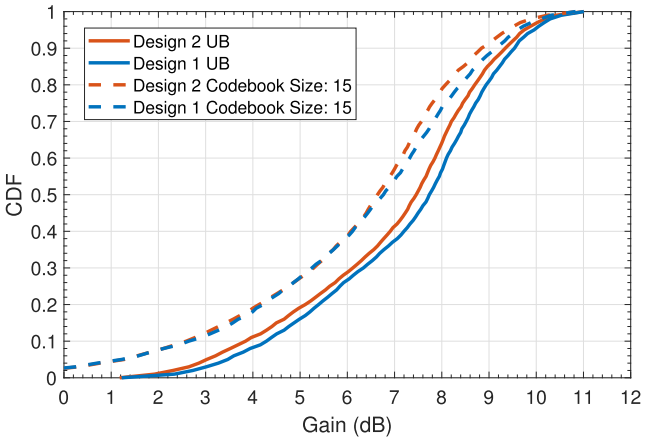

FIGURE 7. The CDF of the spherical coverage of the two mobile phone designs shown in Fig. 1. The solid curves are found assuming the upper bound and the dashed one are for the practical codebook.

coverage is expected since the regions covered by adding the new modules are already mostly covered by the existing modules as can be seen in Fig. 1, which at first glance might imply that having only the antenna modules in the 2^{nd} design is enough since the minor enhancement comes at the expense of adding three new modules (8 antennas) which increases the power consumption, raises the overhead of beam management, and the new modules also have to compete for physical space with other modules in the phone (speakers, camera, buttons, etc.). However, our argument in this work is that the designer should not only look at the free space case (no blockage) while designing the codebook, but also take into account the possible blockage due to hand grips.

To show this, we show the ratio between the 20^{th} (50^{th}) percentile of the spherical coverage of the 1^{st} design over the 2^{nd} design in Table 5, where a different codebook is specifically designed for each grip. It is clear from the table that adding more modules can significantly enhance the performance depending on the hand grip. Grips that cover the regions $4-6$ in Fig. 5, for example, Grip 5 and Grip 14 do not benefit from adding the new modules since these regions are already blocked. However, for other grips (10 and 13 for example), the 1^{st} design can provide more than double the spherical coverage in terms of both, the 20^{th} and the 50^{th} percentiles. This gain can be used to enhance the link quality or to save the power of the mobile device.

TABLE 5. The ratio between the 20^{th} (50^{th}) percentile of the spherical coverage of design 1 over design 2.

Grip ID	20^{th} PCTL Ratio	50^{th} PCTL Ratio
Grip 1	1.02	1.02
Grip 2	1.16	1.10
Grip 3	1.49	1.32
Grip 4	1.31	1.20
Grip 5	1.20	1.10
Grip 6	1.12	1.10
Grip 7	1.29	1.45
Grip 8	2.72	3.35
Grip 9	1.47	1.16
Grip 10	1.21	1.11
Grip 11	2.54	2.77
Grip 12	1.00	1.00
Grip 13	1.53	1.29
Grip 14	1.00	1.00

The takeaway message from this section is that the designer should take the possible hand grips into account while placing the antennas on the mobile device, since a not-so-careful design, i.e., a design based on the free space propagation without considering hand blockage, leads to a significant drop in the performance. This also motivates the next section which shows how to account for the hand grips in the codebook design.

B. DIFFERENT ADAPTATION SCHEMES

In this section, we change our focus from specific hand grips to activities, where each activity can have multiple hand grips with certain probabilities. We use our own data shown in Table 3 and Table 4 as an example and focus on the first mobile design since it is more resilient to hand grips. The 20^{th}, 50^{th}, and 80^{th} percentiles of the spherical coverage are shown in Fig. 8, Fig. 9, and Fig. 10, respectively, for the three codebook adaptation schemes discussed previously. The results are found as follows.

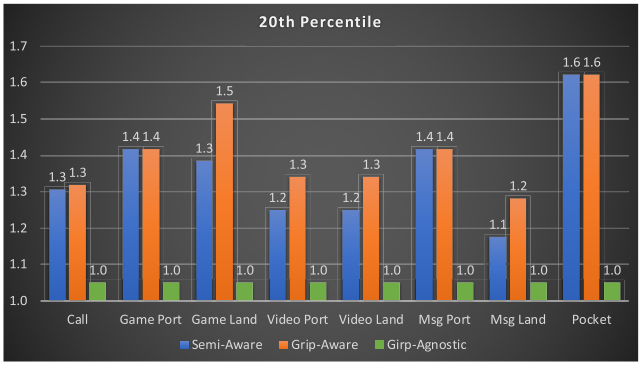

FIGURE 8. The weighted mean of 20^{th} percentile of the spherical coverage for different activities and different codebook adaptation schemes.

For the *Grip-Agnostic* scheme, the codebook is designed based on the radiation vectors of the no blockage case, i.e., the same codebook found in Fig. 7. Then the performance of this codebook is evaluated for each hand grip in Table 3, in terms of the spherical coverage. Hence, we have 15 different sets of data which represents the spherical coverage for each grip assuming the no blockage codebook. Then, for each activity, the weighted mean of the percentiles, based on Table 4, is found and shown in the figures 8, 9, and 10. For the *Grip-Aware* scheme, a codebook is designed for each hand grip, and then the spherical coverage is found for each grip assuming the codebook that is specifically designed for it. The shown percentiles for the different activities are also the weighted mean of the percentiles for each grip. Finally, for the *Semi-Aware* scheme, a single codebook is designed for each activity as described in Section IV. Then for each activity, the spherical coverage distributions are evaluated

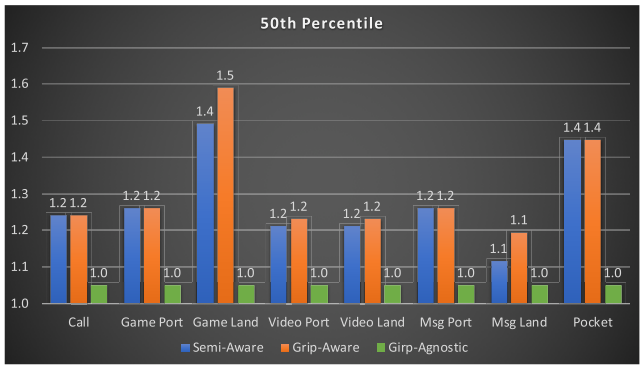

FIGURE 9. The weighted mean of 50^{th} percentile of the spherical coverage for different activities and different code adaptation schemes.

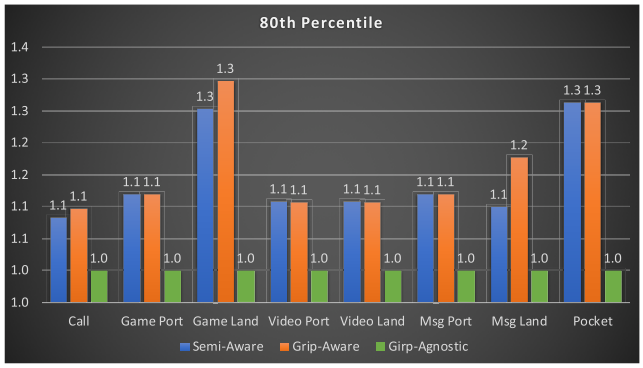

FIGURE 10. The weighted mean of 80^{th} percentile of the spherical coverage of the different activities and different codebook adaptation schemes.

for the activity's corresponding grips assuming the codebook designed for this activity. The percentiles are found in a similar way to the previous cases. To simplify the comparison, the results are normalized by the *Grip-Agnostic* data, i.e., the results are the gains compared to the *Grip-Agnostic* scheme, where 1 means there is no gain.

First, we start by comparing the *Grip-Aware* scheme, which represents the maximum gain we can obtain by adapting the codebook according to the hand grip, and the *Grip-Agnostic* scheme, which is our benchmark scheme that is based on the no-blockage case. As the figures show, we get a considerable gain that ranges between 23% to 57% at 20^{th} percentile by adapting the codebook according to the user hand grip. We also see gains at the 50^{th} and the 80^{th} percentiles. However, an improvement of the 20^{th} percentile is more important for coverage, since it corresponds to the regions where we have a low signal quality, and the user might have a link-failure in case the signal comes from these regions. Additionally, note that the gap between the *Grip-Aware* and the *Grip-Agnostic* schemes varies depending on the activity. In general, the more elements are blocked by the grips, the more benefits brought by adapting the codebook. Hence, for the activities that have grips blocking many elements, the gap between the two schemes is larger. These results also show that the designer does need to take the hand grip into account not only while designing and placing the antennas on the mobile device as discussed in the previous section, but also while designing the beam codebook. A careful codebook design by taking the hand grips into account is necessary and results in a significant performance gain.

However, the obtained gains from the *Grip-Aware* scheme may be unrealistic given the current mobile devices, since it is based on the assumption that the mobile device can accurately detect the user hand grip and this feature is not available in the current mobile phones. Moreover, the beam codebook switching based on the grip may result in high overheads that reduce the gain obtained from this scheme. Hence, we compare the *Grip-Aware* scheme with the proposed *Semi-Aware* scheme, since it is a practical scheme that only requires the knowledge of the application the user is using and the orientation of the phone. Moreover, since the same codebook is used for each activity, the switching overheads mentioned previously are significantly reduced.

The results show that the *Semi-Aware* scheme provides gains ranging between 13% and 57% in terms of the 20^{th} percentile, which are less compared to the gains offered by the *Grip-Aware*, but are still significant compared to the *Grip-Agnostic* scheme. The variation in the gap between the *Semi-Aware* and the *Grip-Agnostic* schemes can be explained in the same way we explained the gap between the *Grip-Aware* and the *Grip-Agnostic* schemes. The variation in the gap between the *Grip-Aware* and the *Semi-Aware* schemes can be explained as follows: the gap is smaller for the activities that have highly correlated grips. Of course, in the cases where there is only one grip, as in the case of the *Msg Portrait*, *Game Portrait*, and *Pocket* activities, the performance of the two schemes is exactly the same. Conversely, for the case of the *Call* activity, the performance is very close due to the high correlation between the different grips obtained for the Call activity as shown in Table 4. Overall, the result shows that we can still harvest performance gains with just the knowledge of the application and the mobile orientation.

C. DISCUSSION AND FUTURE WORK

Firstly, note that the algorithms and schemes presented in this work are universal, but the results are specific for the mobile designs we considered and our data on the different hand grips. In other words, the exact gains from the code adaptation schemes depend on the mobile design and the data about the different hand grips and activities. Nonetheless, our mobile designs are based on the proposals in 3GPP meetings [13]–[15] and our own experiments. Regarding the hand grip data set, our data is based on a small number of participants, eight users, since the purpose is to provide proof of the concept that the hand grip effect plays a key role in the antenna placement on the mobile device and the beam codebook design. Larger data sets will provide more accurate information about the gains obtained by the codebook adaptation schemes we discussed. We have focused on the Greedy algorithm to design the codebooks, but the idea behind the different codebook adaptation schemes still holds even if the designer chooses a different codebook design algorithm. Our

choice of the Greedy algorithm is based on our work in [8], where we show that it performs comparably well as other more sophisticated algorithms.

Secondly, we have focused on the offline design of beam codebook, i.e., the codebooks are designed and stored in the mobile device, and the mobile device just switches between the different codebooks. Another approach is online design, where the codebook is designed dynamically based on the information we can collect from different modules of the phone, i.e., the camera, the gyroscope, proximity sensors, the touch screen, etc. This information can be combined together to design a codebook or adapt the current one to be more suitable for the current environment. In this regard, our offline design of the codebook can serve as the baseline codebook that the device uses, but can adapt it according to the current situation. An online design has the added benefit of converging to codebooks that are user-specific, since different users have different hand grips based on their habits. Regardless of benefits, the online design requires heavy processing of the information and the radiation data, and hence, may not be totally feasible at this time. More likely, the online approach will be used to adapt the offline codebook based on the environment, where tools from machine learning can be deployed.

VI. CONCLUSION

This paper provides a comprehensive analyses on the effect of the user hand grip on the mobile design in terms of the antenna placement and beam codebooks design. More specifically, we compare different mobile designs in terms of the antenna layouts and we show the dramatic impact of the hand blockage on the antenna radiation patterns as well as the spherical coverage. Hence, although different designs can have a similar performance in free space propagation, the performance can be quite different in the presence of hand blockage. In the second part of this work, we show that having some knowledge about the user hand grip can substantially influence the analog beam codebook design and significantly enhance the spherical coverage of the mobile device.

REFERENCES

[1] T. S. Rappaport *et al.*, "Millimeter wave mobile communications for 5G cellular: It will work!" *IEEE Access*, vol. 1, pp. 335–349, May 2013.

[2] W. Hong, K.-H. Baek, Y. Lee, Y. Kim, and S.-T. Ko, "Study and prototyping of practically large-scale mmWave antenna systems for 5G cellular devices," *IEEE Commun. Mag.*, vol. 52, no. 9, pp. 63–69, Sep. 2014.

[3] V. Raghavan *et al.* (2018). "Statistical blockage modeling and robustness of beamforming in millimeter wave systems." [Online]. Available: https://arxiv.org/abs/1801.03346

[4] *Title 47 Code of Federal Regulations Part 2*, Federal Commun. Commission, Washington, DC, USA, Feb. 1093.

[5] *Title 47 Code of Federal Regulations Part 1*, Federal Commun. Commission, Washington, DC, USA, Jan. 1310.

[6] V. Raghavan, A. Partyka, L. Akhoondzadeh-Asl, M. A. Tassoudji, O. H. Koymen, and J. Sanelli, "Millimeter wave channel measurements and implications for PHY layer design," *IEEE Trans. Antennas Propag.*, vol. 65, no. 12, pp. 6521–6533, Dec. 2017.

[7] A. Alkhateeb, J. Mo, N. Gonzalez-Prelcic, and R. W. Heath, Jr., "MIMO precoding and combining solutions for millimeter-wave systems," *IEEE Commun. Mag.*, vol. 52, no. 12, pp. 122–131, Dec. 2014.

[8] J. Mo *et al.*, "Beam codebook design for 5G mmWave terminals," *IEEE Access*, submitted for publication.

[9] V. Raghavan, M.-L. C. Chi, M. A. Tassoudji, O. H. Koymen, and J. Li, "Antenna placement and performance tradeoffs with hand blockage in millimeter wave systems," *IEEE Trans. Commun.*, vol. 67, no. 4, pp. 3082–3096, Apr. 2019.

[10] *Study on Channel Model for Frequencies From 0.5 to 100 GHz (Release 14)*, document 3GPP TR 38.901, Sep. 2017.

[11] K. Zhao, J. Helander, Z. Ying, D. Sjoberg, M. Gustafsson, and S. He, "mmWave phased array in mobile terminal for 5G mobile system with consideration of hand effect," in *Proc. IEEE Veh. Technol. Conf.*, May 2015, pp. 1–4.

[12] R. Khan, A. A. Al-Hadi, and P. J. Soh, "Efficiency of millimeter wave mobile terminal antennas with the influence of users," *Prog. Electromagn. Res.*, vol. 161, pp. 113–123, Apr. 2018.

[13] *Consideration of EIRP Spherical Coverage Requirement*, document R4-1711036, 3GPP TSG-RAN WG4 Meeting 84, Samsung, Apple, Intel, Oct. 2017.

[14] *Consideration of EIRP Spherical Coverage Requirement*, document R4-1713850, 3GPP TSG-RAN WG4 Meeting 85, Apple Intel, Nov. 2017.

[15] *Spherical Coverage of Realistic Design*, document R4-1712381, 3GPP TSG-RAN WG4 Meeting 85, Qualcomm Incorporated, Nov. 2017.

[16] *Ansoft High Frequency Structure Simulation (HFSS) Version 13*, Ansoft Corp., Pittsburgh, PA, USA, 2010.

[17] I. Syrytsin, S. Zhang, and G. F. Pedersen, "User impact on phased and switch diversity arrays in 5G mobile terminals," *IEEE Access*, vol. 6, pp. 1616–1623, 2018.

[18] R. Swinbank and R. J. Purser, "Fibonacci grids: A novel approach to global modelling," *Quart. J. Roy. Meteorol. Soc.*, vol. 132, no. 619, pp. 1769–1793, 2006.

[19] M. Peter *et al.*, "Analyzing human body shadowing at 60 GHz: Systematic wideband MIMO measurements and modeling approaches," in *Proc. Eur. Conf. Antennas Propag. (EUCAP)*, Mar. 2012, pp. 468–472.

[20] K. R. Boyle, Y. Yuan, and L. P. Ligthart, "Analysis of mobile phone antenna impedance variations with user proximity," *IEEE Trans. Antennas Propag.*, vol. 55, no. 2, pp. 364–372, Feb. 2007.

[21] A. A.-H. Azremi *et al.*, "Coupling element-based dual-antenna structures for mobile terminal with hand effects," *Int. J. Wireless Inf. Netw.*, vol. 18, no. 3, pp. 146–157, 2011.

[22] C. H. Li, E. Ofli, N. Chavannes, and N. Kuster, "Effects of hand phantom on mobile phone antenna performance," *IEEE Trans. Antennas Propag.*, vol. 57, no. 9, pp. 2763–2770, Sep. 2009.

[23] C. H. Li, M. Douglas, E. Ofli, N. Chavannes, Q. Balzano, and N. Kuster, "Mechanisms of RF electromagnetic field absorption in human hands and fingers," *IEEE Trans. Microw. Theory Techn.*, vol. 60, no. 7, pp. 2267–2276, Jul. 2012.

[24] D. Andreuccetti. (2012). *An Internet Resource for the Calculation of the Dielectric Properties of Body Tissues in the Frequency Range 10 Hz-100 GHz*. [Online]. Available: http://niremf.ifac.cnr.it/tissprop/

[25] T. M. Greiner, "Hand anthropometry of U.S. army personnel," Army Natick Res. Develop. Eng. Center, Natick, MA, SA, Tech. Rep. ADA244533, 1991.

[26] S. Hoober, "How do users really hold mobile devices," *UXmatters: Insights Inspiration User Exper. Community*, Feb. 2013.

[27] K. Hinckley, J. Pierce, M. Sinclair, and E. Horvitz, "Sensing techniques for mobile interaction," in *Proc. ACM Symp. User Interface Softw. Technol.*, 2000, pp. 91–s100.

[28] K.-E. Kim *et al.*, "Hand grip pattern recognition for mobile user interfaces," in *Proc. Nat. Conf. Artif. Intell.*, vol. 21, no. 2. Cambridge, MA, USA: MIT Press, 2006, p. 1789.

AHMAD ALAMMOURI (S'11) received the B.Sc. degree (Hons.) in electrical engineering from The University of Jordan, Amman, Jordan, in 2014, and the M.Sc. degree in electrical engineering from the King Abdullah University of Science and Technology (KAUST), Thuwal, Saudi Arabia, in 2016. He is currently pursuing the Ph.D. degree with the Department of Electrical and Computer Engineering, The University of Texas at Austin, Austin, TX, USA. He has held summer internships at Samsung Research America, Richardson, TX, USA, from 2017 to 2018. His research interests include statistical modeling and performance analysis of wireless networks.

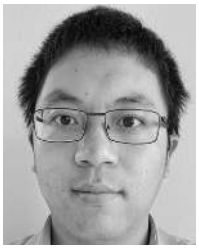

JIANHUA MO (S'12–M'17) received the B.S. and M.S. degrees from Shanghai Jiao Tong University, in 2010 and 2013, respectively, and the Ph.D. degree from The University of Texas at Austin, in 2017, all in electrical engineering.

He is currently a Staff Engineer with Samsung Research America, Plano, TX, USA. His research interests include physical layer security and MIMO communications with low-resolution ADCs. He is also involved in the development of mmWave wireless backhaul transmission and 5G UE beam codebook. His awards and honors include the Heinrich Hertz Award for best IEEE COMMUNICATIONS LETTERS, in 2013, the Exemplary Reviewer of the IEEE WIRELESS COMMUNICATIONS LETTERS, in 2012, the Finalist for the Qualcomm Innovation Fellowship, in 2014, and the Exemplary Reviewer of the IEEE COMMUNICATIONS LETTERS, in 2015.

BOON LOONG NG received the B.E. (Electrical and Electronic) degree and the Ph.D. degree in engineering from the University of Melbourne, Australia, in 2001 and 2007, respectively. He is currently the Research Director of the Standards and Mobility Innovation (SMI) Lab, Samsung Research America, Plano, TX, USA. He had contributed to 3GPP RAN L1/L2 standardizations of LTE, LTE-A, LTE-A Pro, and 5G NR technologies, from 2008 to 2018. Since 2018, he has been leading a R&D team that develops system and algorithm design solutions for commercial 5G and Wi-Fi technologies. He holds over 60 USPTO-granted patents on LTE/LTE-A/LTE-A Pro/5G and more than 100 patent applications globally.

JIANZHONG CHARLIE ZHANG (F'16) received the Ph.D. degree from the University of Wisconsin–Madison. From 2009 to 2013, he has served as the Vice Chairman of the 3GPP RAN1 working group and led development of LTE and LTE-Advanced Technologies, such as 3D channel modeling, UL-MIMO, CoMP, and Carrier Aggregation for TD-LTE. He is also the VP and the Head of the Standards and Mobility Innovation Lab, Samsung Research America, where he leads research, prototyping, and standards for 5G and future multimedia networks.

JEFFREY G. ANDREWS (S'98–M'02–SM'06–F'13) received the B.S. degree (Hons.) in engineering from Harvey Mudd College and the M.S. and Ph.D. degrees in electrical engineering from Stanford University.

He developed Code Division Multiple Access systems at Qualcomm, from 1995 to 1997. He has served as a Consultant to Samsung, Nokia, Qualcomm, Apple, Verizon, AT&T, Intel, Microsoft, Sprint, and NASA. He is currently the Cullen Trust Endowed Professor (#1) of ECE with The University of Texas at Austin. He is the coauthor of the books: *Fundamentals of WiMAX* (Prentice-Hall, 2007) and *Fundamentals of LTE* (Prentice-Hall, 2010). He is also a member of the Technical Advisory Board of Artemis Networks and GenXComm. He was a co-recipient of 15 paper awards, including the 2010 IEEE ComSoc Best Tutorial Paper Award, the 2011 and 2016 IEEE Heinrich Hertz Prizes, the 2014 IEEE Stephen O. Rice Prize, the 2014 and 2018 IEEE Leonard G. Abraham Prizes, and the 2016 IEEE Communications Society & Information Theory Society Joint Paper Award. He received the 2015 Terman Award, the NSF CAREER Award, and the 2019 IEEE Kiyo Tomiyasu Technical Field Award. He is also the Chair of the IEEE Communications Society Emerging Technologies Committee. He is also an ISI Highly Cited Researcher. He was the Editor-in-Chief of the IEEE TRANSACTIONS ON WIRELESS COMMUNICATIONS, from 2014 to 2016.